

## Adsorption of NH<sub>3</sub> and NO<sub>2</sub> on Single-Walled Carbon Nanotubes

Mark D. Ellison,\* Michael J. Crotty, Dukho Koh, Ryan L. Spray, and Kaitlin E. Tate

Department of Chemistry, Wittenberg University, Springfield, Ohio 45501

Received: February 12, 2004; In Final Form: April 1, 2004

The interaction of NH<sub>3</sub> and NO<sub>2</sub> with heterogeneous bundles of carbon single-walled nanotubes (SWNTs) has been studied using FTIR spectroscopy and temperature-programmed desorption (TPD). Both NH<sub>3</sub> and NO<sub>2</sub> adsorb at room temperature, and the interaction results in strong shifts of the vibrational modes of the molecules relative to the gas phase. The data suggest that NH<sub>3</sub> adsorbs via both its lone pair and its H atoms. NO<sub>2</sub> adsorbs in an asymmetric configuration via at least one of the oxygen atoms. Analysis of the IR data suggests that these molecules adsorb by interacting with multiple nanotubes within a bundle of SWNTs. Additionally, trimethylamine, a compound similar to NH<sub>3</sub>, does not adsorb at room temperature. It is postulated that the size of trimethylamine prevents it from entering the grooves between nanotubes in the sample, whereas NH<sub>3</sub> and NO<sub>2</sub> are small enough to enter the grooves and interact with multiple nanotubes.

### Introduction

Since their discovery in 1991, carbon nanotubes<sup>1</sup> have been the subject of intense study. Because of their inherent ability to conduct electricity, much effort has been devoted to integrating nanotubes into microelectronic devices. A recent study by Kong et al.<sup>2</sup> demonstrated that exposure to NH<sub>3</sub> or NO<sub>2</sub> gas could dramatically alter the conductivity of single-walled nanotubes (SWNTs). Additionally, it has been clearly demonstrated that O<sub>2</sub> also affects the electrical properties of SWNTs.<sup>3</sup> These investigations, however, did not determine the nature of the interaction between the gas molecules and the SWNTs. Computational studies<sup>4–6</sup> have shed some light on the interaction of small molecules with SWNTs, but experimental data have not yet been presented. Certainly, a more detailed understanding of the nature of the interaction of gases with SWNTs is necessary if the gases are to be used to tailor the physical properties of the SWNTs.

The adsorption of gases on and in carbon nanotubes at low temperatures has been extensively studied. Hydrogen is of particular interest for energy applications. Additionally, the physisorption of Xe<sup>7,8</sup> and CF<sub>4</sub><sup>9</sup> has recently been examined. The adsorption of gases, particularly CH<sub>4</sub>, C<sub>2</sub>H<sub>2</sub>, C<sub>2</sub>H<sub>4</sub>, CH<sub>3</sub>OH,<sup>10</sup> CO and NO;<sup>11</sup> and NH<sub>3</sub><sup>12</sup> on a similar substrate, C<sub>60</sub>, has also been studied. For CH<sub>4</sub>, C<sub>2</sub>H<sub>2</sub>, C<sub>2</sub>H<sub>4</sub>, CO, and NO, the adsorption was shown to be caused by dispersion forces (i.e., physisorption). Because of the weakness of the interaction, these gases would adsorb only below room temperature. CH<sub>3</sub>OH and NH<sub>3</sub> showed stronger interactions, and NH<sub>3</sub> was postulated to adsorb by sharing the lone pair on the N atom with C<sub>60</sub>. Still, NH<sub>3</sub> did not adsorb unless the C<sub>60</sub> substrate was cooled below room temperature. It is noteworthy that any of these molecules could adsorb by entering cavities between C<sub>60</sub> molecules and interacting with multiple cages. Still, to the best of our knowledge, no studies have been carried out with gases that interact strongly with SWNTs.

In addition to affecting the electrical properties, small gas molecules provide an opportunity to study the chemistry of nanotubes. To be integrated effectively into devices, SWNTs

must be functionalized, so much effort has been put forth to achieve this goal. The interaction of gas molecules with SWNTs represents an opportunity to learn about the chemical reactivity of SWNTs. Therefore, we have undertaken the task of elucidating the interaction between small molecules and SWNTs. This work was specifically motivated by the results of Kong et al.<sup>2</sup> for NH<sub>3</sub> and NO<sub>2</sub> interacting with an SWNT.

### Experimental Section

Single-walled carbon nanotubes produced by the HiPCO process were purchased from Carbon Nanotechnologies, Inc. These are provided at 95% purity and were used as received. Most published purification techniques<sup>13–17</sup> involve strongly oxidizing conditions that have been shown to remove the end caps and oxidize the walls of the nanotubes.<sup>18</sup> We wished to avoid the complication of the possibility of gas molecules on the inside of the nanotubes, so we did not use these purification methods. Our attempts at more benign purification schemes<sup>19</sup> were unsuccessful, likely because of aggregation of the SWNTs into bundles.<sup>20</sup> The major impurity in HiPCO SWNTs is graphite-covered iron particles. Because the gases of interest do not adsorb on graphite at room temperature,<sup>21,22</sup> these impurities are not expected to affect our results.

FTIR spectra were obtained with a Mattson Research Series FTIR spectrometer using a liquid nitrogen cooled HgCdTe detector. The vacuum cube was placed into the nitrogen-purged sample compartment of the spectrometer so that the data were acquired in transmission mode. Typically, 1000–2000 scans were averaged, and the resolution was 1 cm<sup>-1</sup>.

SWNTs were wetted with toluene or DMF and pressed onto a tungsten screen (Buckbee-Mears, >85% optical transmission). The resulting nanotube layer was uniform and had a thickness of ~1 mm. The screen was mounted in a stainless steel vacuum cube with ZnSe windows. A base pressure of 4 × 10<sup>-7</sup> Torr in the cube was achieved using a liquid nitrogen sorption pump and a 30 L/s ion pump (Varian). The SWNTs were heated to about 725 K by running current through the tungsten screen. This process desorbs atmospheric gases, including O<sub>2</sub> and H<sub>2</sub>O, and the solvent used to wet the nanotubes for deposition on the screen. In addition, this temperature should be sufficient to

\* Corresponding author. E-mail: mellison@wittenberg.edu.

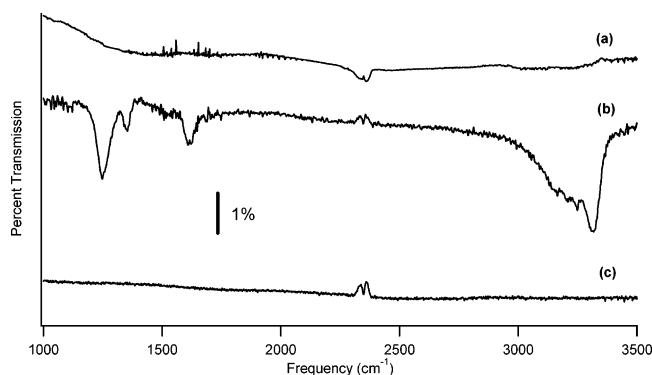


**Figure 1.** FTIR spectra of (a) bare nanotubes, (b) ammonia adsorbed on SWNTs, and (c) nanotubes after exposure to trimethylamine.

desorb carboxylic functional groups from the SWNTs.<sup>18</sup> Heating was applied for at least 12 h to drive out all gases. Once the heating was ceased, the SWNTs were allowed to cool to room temperature before being exposed to gases.

Trace a of Figure 1 shows a spectrum acquired of the bare nanotubes after heating as described above. Peaks around 1600 and 2300 cm<sup>-1</sup> are due to the incomplete cancellation of absorbance by water vapor and carbon dioxide, respectively, in the spectrometer sample chamber. We note that this spectrum is similar to an ATR-IR spectrum of SWNTs published in a study of fluorination of nanotubes.<sup>23</sup> Yates et al. have demonstrated that, unless heated, SWNTs have carboxylic acid and quinine-like functional groups on the walls.<sup>18</sup> These functional groups were identified by characteristic vibrational peaks at 1245 cm<sup>-1</sup> [ $\nu(\text{C}-\text{O})$ ], 1660 cm<sup>-1</sup> [ $\nu(\text{C}=\text{O})$  quinine], and 1735 cm<sup>-1</sup> [ $\nu(\text{C}=\text{O})$  acid]. The absence of such features in trace a strongly suggests that the heating procedure removed these functional groups.

NH<sub>3</sub> (Matheson, 99.5%). NO<sub>2</sub> (Praxair, 99.9%). and N(CH<sub>3</sub>)<sub>3</sub> (Aldrich, 99%) gases were passed through a drying tube of 3A molecular sieve, alumina, and NaOH to remove traces of water vapor. Exposure pressures could not be accurately measured, because Convector gauge (Granville-Philips) calibration data for these gases do not exist. We performed our own rough calibration and estimate that the gas pressures during exposure were on the order of 50 Torr. Exposure times ranged from 5 to 15 min. After exposure to the gas, the cube was purged for 15 min with dry nitrogen to remove any traces of gaseous reactant.

We have also carried out temperature-programmed desorption (TPD) studies of gases adsorbed on SWNTs. In these experiments, the SWNTs were pressed onto a tungsten screen in the same manner as described above. The SWNTs were placed in a vacuum chamber equipped with a quadrupole mass spectrometer (Stanford Research Systems RGA100) and a leak valve. The SWNTs were exposed to a net pressure (above the base pressure of the chamber) of  $6 \times 10^{-7}$  Torr of gas for 25 s to give an exposure of 15 L. The SWNTs were heated at a rate of 2 K/s by running current through the tungsten screen, and the mass spectrometer was used to measure the partial pressures of the gases evolved. Temperature measurements were made using a type K thermocouple attached to the screen and referenced to an ice bath. The heating, temperature measurements, and mass spectrometer were controlled by LabView software, and the accuracy of the temperature measurements was  $\pm 3$  K.

## Results

Trace b of Figure 1 shows the FTIR data for NH<sub>3</sub> adsorbed on SWNTs. Such spectra are quite reproducible, and we note that virtually identical spectra can also be obtained by heating

**TABLE 1: Vibrational Frequencies (cm<sup>-1</sup>) for NH<sub>3</sub> on SWNTs and in Relevant Systems**

vibrational mode	SWNTs	gas phase (ref 39)	C <sub>60</sub> (ref 12)	dissolved in benzene
$\nu_3$ (asymmetric stretch)	3318, 3249	3414	3354	3145
$\nu_1$ (symmetric stretch)	3205, 3156	3337.5, 3336	3222	
$\nu_2$ (bend)	1618	1627	1616	1728
$\nu_4$ (umbrella)	1354, 1248	968, 932	1132	1282

the SWNTs in a vacuum and then exposing them to NH<sub>3</sub> again. A broad feature with a maximum at 3318 cm<sup>-1</sup> and three distinct shoulders is assigned to the N-H stretching vibrations. The peak at 1618 cm<sup>-1</sup> is assigned to the N-H bend, and the peak at 1248 cm<sup>-1</sup> with the small feature to slightly higher frequency is the symmetric deformation ("umbrella" mode). The small feature at  $\sim 2300$  cm<sup>-1</sup> arises from incomplete cancellation of CO<sub>2</sub> in the spectrometer during the background and sample scans. The N-H stretch and N-H bend vibrations are both red-shifted with respect to the corresponding features for gas-phase ammonia. However, the umbrella mode is blue-shifted by about 300 cm<sup>-1</sup>. Additionally, the peaks are significantly broader than in the gas phase, and no rotational structure is observed. This indicates that the NH<sub>3</sub> observed is interacting with the SWNTs. A comparison of these peak frequencies to those in relevant systems is presented in Tables 1 and 2. All modes except the umbrella mode agree fairly well with the reported frequencies for NH<sub>3</sub> adsorbed on buckminsterfullerene, C<sub>60</sub>. Similar agreement is also noted for the metal ion complexes. In these systems, NH<sub>3</sub> acts as an electron donor. That is, it shares the lone pair on the N atom with C<sub>60</sub> or the Mg<sup>2+</sup> ion, respectively. In contrast, for NH<sub>3</sub>/benzene clusters<sup>24-27</sup> and for NH<sub>3</sub> dissolved in benzene, ammonia is believed to interact with benzene via the H atoms. For these systems, the interaction is similar to hydrogen bonding, with one or more H atoms overlapping with the  $\pi$  electrons of the ring. Thus, we collected an FTIR spectrum of ammonia dissolved in benzene, and those peak frequencies are also included in Table 1. Comparing these data to our results for ammonia adsorbed on SWNTs, it is apparent that the umbrella-mode frequency agrees well, but the frequencies of the rest of the modes do not.

To help clarify these results, we also exposed the SWNTs to trimethylamine, N(CH<sub>3</sub>)<sub>3</sub>. This molecule is similar to ammonia in that both have a lone pair of electrons on the N atom. However, trimethylamine has three methyl groups in place of three H atoms. Because hydrocarbons do not adsorb on SWNTs at room temperature,<sup>28,29</sup> trimethylamine is expected to be able to interact with SWNTs only via the lone pair on the N atom. The FTIR spectra collected, an example of which is shown in trace c of Figure 1, showed no peaks corresponding to trimethylamine, indicating that this molecule does not adsorb on SWNTs at room temperature. TPD studies show no desorption of trimethylamine or any fragments from SWNTs. These results bolster the conclusion from the FTIR experiments that trimethylamine does not adsorb on SWNTs at 300 K.

Figure 2 shows a representative FTIR spectrum for SWNTs exposed to NO<sub>2</sub>. Again, such spectra were also reproducibly obtained by heating the SWNTs in a vacuum and exposing them to NO<sub>2</sub>. The region from 1400 to 1800 cm<sup>-1</sup> is shown for purposes of discussion. However, all peaks in this region are attributable to incomplete cancellation of absorbances due to water vapor in the spectrometer. At lower frequencies, three features are noted at 1302, 1026, and 808 cm<sup>-1</sup>. These peaks are broader, and all but the 808 cm<sup>-1</sup> feature are shifted to lower frequencies than those of gas-phase NO<sub>2</sub>. Thus, they provide evidence that the molecules are adsorbed on the SWNTs. The two peaks at higher frequencies are due to N-O stretches, and

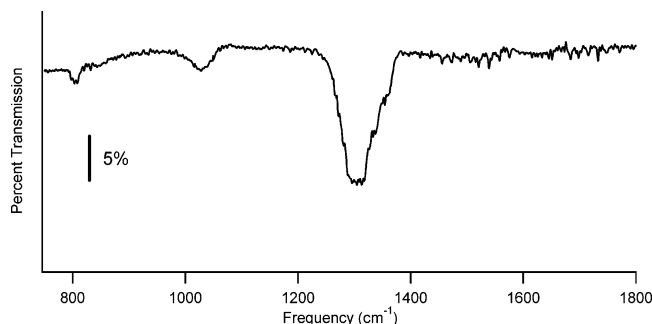
**TABLE 2: Vibrational Frequencies (cm<sup>-1</sup>) for NH<sub>3</sub> on SWNTs, in Transition Metal Complexes, and Adsorption on Metal Surfaces<sup>a</sup>**

vibrational mode	SWNTs	solid-phase NH <sub>3</sub> (ref 40)	M(NH <sub>3</sub> ) <sub>6</sub> <sup>3+</sup> (ref 30) <sup>b</sup>	M(NH <sub>3</sub> ) <sub>6</sub> <sup>2+</sup> (ref 30) <sup>c</sup>	adsorbed on metal surfaces <sup>d</sup>
$\nu_3$ (asymmetric stretch)	3318, 3249	3378	3269 (3) 3240–3310	3338 (7) 3315–3353	3364 (6) 3340–3400
$\nu_1$ (symmetric stretch)	3205, 3156	3290	3183 (3) 3130–3250	3202 (7) 3175–3250	3263 (6) 3200–3320
$\nu_2$ (bend)	1618	1650	1616 (6) 1587–1630	1601 (8) 1585–1612	1610 (7) 1580–1648
$\nu_4$ (umbrella)	1354, 1248	1060	1333 (6) 1290–1369	1158 (8) 1091–1220	1118 (7) 1050–1170

<sup>a</sup> For the comparison systems, the first number represents the average value for that vibrational frequency. The value in parentheses is the number of compounds that were used in computing the average. Below the average is the range of values for that vibrational mode. <sup>b</sup> Data are for M = Cr, <sup>50</sup>Cr, Ru, Co, Rh, and Ir. <sup>c</sup> Data are for M = Mg, Mn, Fe, Ru, Co, Ni, Zn, and Cd. <sup>d</sup> Data are for Ag(110), Ag(311), Pt(111), Ni(111), Ni(110), Fe(110), and Ru(0001). See ref 31 and references therein.

**TABLE 3: Vibrational Frequencies (cm<sup>-1</sup>) for NO<sub>2</sub> on SWNTs and in Relevant Systems**

vibrational mode	gas phase (ref 39)	SWNTs	NO <sub>2</sub> /Au(111) (ref 36)	Ni(py) <sub>4</sub> (ONO) <sub>2</sub> (ref 30)	Gaseous N <sub>2</sub> O <sub>4</sub> (ref 39)
$\nu_{as}$ (asymmetric stretch)	1618	1302	—	1393 $\nu$ (N=O)	1758
$\nu_{ss}$ (symmetric stretch)	1318	1026	1178	1114 $\nu$ (N–O)	1261
$\delta$ (bend)	750	808	805	825	755

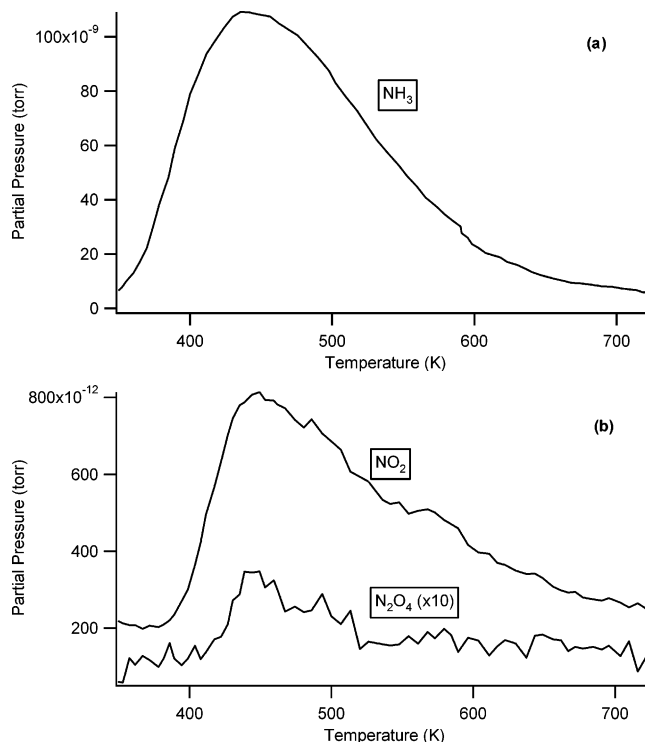
**Figure 2.** FTIR spectrum of NO<sub>2</sub> adsorbed on SWNTs.

the peak at 808 cm<sup>-1</sup> is due to the bending motion. A summary of these peak frequencies and relevant comparison systems is presented in Table 3.

Figure 3 shows the TPD data for (a) NH<sub>3</sub> and (b) NO<sub>2</sub> adsorbed on SWNTs. Control experiments indicate that the gases are desorbing from the SWNTs and not the screen or the sample holder. The data for NH<sub>3</sub> are corrected for the presence of water background in the chamber. The measurement of mass 17 shows a peak at a temperature of 430 K. We did not observe evidence for the desorption of any other species that could be produced by decomposition of NH<sub>3</sub>. The NO<sub>2</sub> data are similar, with a mass 46 peak at 450 K. A very small amount of mass 92 (N<sub>2</sub>O<sub>4</sub>) was also observed, as shown in Figure 3b. The large widths of the two desorption features could be indicative of molecules adsorbed between SWNTs in a bundle. However, they could also be caused by the relatively low pumping speed of the system.

## Discussion

**Ammonia.** The vibrational data obtained for SWNTs exposed to NH<sub>3</sub> are consistent with the adsorption of the molecules onto the nanotubes. Specifically, the frequency shifts and broadening all are indicative of an adsorbed species. Additionally, the TPD data show only molecular desorption at a temperature well above room temperature. A comparison of the observed vibrational frequencies to those of solid ammonia (Table 2) shows no similarity. We therefore exclude condensation of a thick film

**Figure 3.** Temperature-programmed desorption data for (a) NH<sub>3</sub> and (b) NO<sub>2</sub> adsorbed on SWNTs. For both experiments the exposure was 15 L.

as a possibility. As shown in Tables 1 and 2, some of the vibrational frequencies are in agreement with those of NH<sub>3</sub> adsorbed on C<sub>60</sub> and on metal surfaces, as well as with those of the metal complexes. In all of these systems, the NH<sub>3</sub> molecules interact via the lone pair on the N atom.<sup>12,30</sup> The strong similarity between our results and these previous measurements suggests that NH<sub>3</sub> also adsorbs on SWNTs via the lone pair. However, two discrepancies must be explained. First, the observed frequency of the umbrella mode for NH<sub>3</sub> adsorbed on SWNTs is more strongly blue-shifted than for the comparison systems. Second, our results for trimethylamine, which is expected to



interact with SWNTs only via the lone pair, showed that this molecule does not adsorb at room temperature.

In their analysis of EELS data for  $\text{NH}_3/\text{Ru}(0001)$ , Parmeter et al. pointed out that, in metal–ammonia complexes, the size of the blue shift of the umbrella mode correlates with increasing charge on the metal ion.<sup>31</sup> This is apparent in Table 2, which shows that the umbrella-mode frequencies in the  $\text{M}^{3+}$  complexes are significantly higher than those in the  $\text{M}^{2+}$  complexes. This trend has also been used to help explain the observed umbrella-mode frequency for ammonia adsorbed on  $\text{Al}(111)\text{--H}$ .<sup>32</sup> Although the umbrella-mode frequency of ammonia in the  $\text{M}^{3+}$  complexes gives better agreement with ammonia adsorbed on SWNTs, the N–H stretch modes of the  $\text{M}^{3+}$  complexes no longer have comparable frequencies. Indeed, we note that, in addition to the previously mentioned positive correlation between umbrella-mode frequency and metal ion charge, there is a negative correlation between the N–H stretching frequency and the metal ion charge. In fact, none of the metal–ammonia complexes in ref 30 show simultaneous good agreement with  $\text{NH}_3/\text{SWNTs}$  for all vibrational frequencies. This suggests that the comparison with these complexes does not encompass the overall adsorption characteristics for  $\text{NH}_3/\text{SWNTs}$ . Furthermore, the C atoms in SWNTs are electrically neutral, and the walls are electron-rich, so a comparison to the interaction of ammonia with highly charged metal ions cannot be sufficient.

Table 2 also shows a comparison of the vibrational frequencies of ammonia adsorbed on SWNTs with those of ammonia adsorbed on various metal surfaces. Investigations of ammonia adsorbed on metal surfaces, including  $\text{Al}(111)$ ,<sup>32</sup>  $\text{Ru}(0001)$ ,<sup>31,33</sup> and  $\text{Ni}(110)$ ,<sup>34</sup> also show a blue shift of the umbrella mode. In these studies, however, the vibrational frequencies are in the range of  $1050\text{--}1170\text{ cm}^{-1}$ , much lower than the observed frequencies for ammonia adsorbed on SWNTs. In adsorption on metal surfaces, ammonia was shown to adsorb to the surface via its lone pair. The discrepancy between the umbrella-mode frequencies for these systems and for ammonia adsorbed on SWNTs suggests that forces in addition to the donation of the lone pair are present in the  $\text{NH}_3/\text{SWNTs}$  system.

Because nanotubes tend to aggregate in bundles, recent calculations and simulations<sup>5,6</sup> have examined the interaction of small gas molecules with multiple SWNTs. These studies have clearly demonstrated that the binding energy is significantly greater for molecules that adsorb at groove sites between two adjacent SWNTs or in interstitial channels between multiple SWNTs than for those that adsorb on the outside of the wall of just one SWNT. We believe that our experimental data are consistent with these findings. An ammonia molecule in a groove site or an interstitial channel would be held more tightly than one on the outside of a single tube, enabling the molecules to remain adsorbed at 300 K. Additionally, a molecule in such a location would have its umbrella motion significantly constrained relative to the gas phase. Thus, the umbrella-mode vibrational frequency is expected to shift to higher frequency, as we observe for ammonia adsorbed on SWNTs.

Studies of benzene/ammonia clusters have shown that the ammonia molecule interacts with the benzene in a hydrogen-bond-like manner, with the H atoms overlapping the  $\pi$  electrons of the benzene ring.<sup>24–27</sup> Because SWNTs also have significant  $\pi$ -electron density, it is reasonable to extrapolate from the cluster studies to the case of  $\text{NH}_3/\text{SWNTs}$ . Attraction between the H atoms of the ammonia molecule and the  $\pi$ -electron density of the SWNTs would also hinder the umbrella vibration of the molecule. This is likely a contributing factor to the observed umbrella-mode frequency for  $\text{NH}_3/\text{SWNTs}$ . Our results show

a similarity in umbrella-mode frequencies for ammonia dissolved in benzene and ammonia adsorbed on SWNTs. Because a comparison to metal–ammonia complexes and adsorption on metal surfaces cannot completely account for the observed vibrational frequencies, we believe that a model in which an ammonia molecule interacts with SWNTs via both ends of the molecule is best suited for explaining these results.

Finally, trimethylamine was not observed to adsorb on SWNTs at 300 K. If ammonia adsorbed solely via the lone pair, then trimethylamine would also be expected to adsorb on SWNTs. Because trimethylamine does not adsorb at 300 K, this suggests that the interaction of  $\text{NH}_3$  involves more facets than just the lone pair. The H atoms are clearly important for overlap with the  $\pi$  electrons of the nanotube wall. Judging from the optimized geometry of heterogeneous bundles of nanotubes used in theoretical studies,<sup>5</sup> the average distance between nanotubes in such a bundle is about  $3.5\text{ \AA}$ . Additionally, ammonia is small enough, with a width of about  $1.6\text{ \AA}$ , to enter into the space between multiple nanotubes. Trimethylamine, however, has a width of roughly  $4.2\text{ \AA}$  and is simply too large to fit in interstitial channels. This indicates that the ability to form hydrogen-bond-like links and the ability to fit between multiple nanotubes are important for the adsorption of ammonia on SWNTs.

Finally, we note that the spectrum in Figure 1 shows a splitting of the umbrella-mode peak and several shoulders on the N–H stretching vibration. The multiple peaks could arise from different adsorption sites on the nanotubes. For instance, theoretical calculations considered the possibility of adsorption over a C atom versus adsorption over the center of a C–C bond or over the center of a hexagonal unit.<sup>6</sup> Additionally, defects in the nanotubes could present alternative sites for adsorption. Finally, because the sample is a mixture of semiconducting and metallic nanotubes, the multiple peaks could arise from adsorption on different types of SWNTs. Clearly, more work is needed to further elucidate these possibilities.

**Nitrogen Dioxide.** The TPD data show that  $\text{NO}_2$  is the primary species desorbed from SWNTs, suggesting that  $\text{NO}_2$  adsorbs molecularly on SWNTs at 300 K. The FTIR data, which show three peaks consistent with adsorbed  $\text{NO}_2$ , support this conclusion. In the gas phase,  $\text{NO}_2$  is in equilibrium with  $\text{N}_2\text{O}_4$ , so adsorption of  $\text{N}_2\text{O}_4$  might also be expected. Furthermore, HREELS studies of the adsorption of  $\text{NO}_2$  on graphite showed that the molecules adsorb as  $\text{N}_2\text{O}_4$ .<sup>22</sup> However, our data show evidence of neither the strong absorbance at  $1790\text{ cm}^{-1}$  that is characteristic of adsorbed  $\text{N}_2\text{O}_4$  nor the numerous other modes of the molecule that are IR-active. The lack of peaks corresponding to  $\text{N}_2\text{O}_4$  in the FTIR spectrum, in conjunction with the TPD data showing desorption of primarily  $\text{NO}_2$ , strongly suggests that the molecules adsorb as  $\text{NO}_2$  at room temperature. On some metal surfaces,  $\text{NO}_2$  adsorbs dissociatively into NO and O atoms, and the NO can interact with adsorbed  $\text{NO}_2$  to form  $\text{N}_2\text{O}_3$ . We observed neither a feature near  $1160\text{ cm}^{-1}$  due to a N–O stretch<sup>35</sup> nor a feature near  $1903\text{ cm}^{-1}$  due to  $\text{N}_2\text{O}_3$ ,<sup>36</sup> indicating that the molecules do not dissociate upon adsorption. Thus, we conclude that the gas adsorbs primarily as individual  $\text{NO}_2$  molecules and neither aggregates into dimers nor dissociates.

The vibrations of the  $\text{NO}_2^-$  ion in various configurations have been well-studied. Several possible interaction geometries are shown in Figure 4. For *nitro* complexes, in which the ion is bound to a metal cation via the N atom, the symmetric and asymmetric stretches have similar frequencies.<sup>37</sup> In contrast, *nitrito* complexes have a broader range of possible bonding

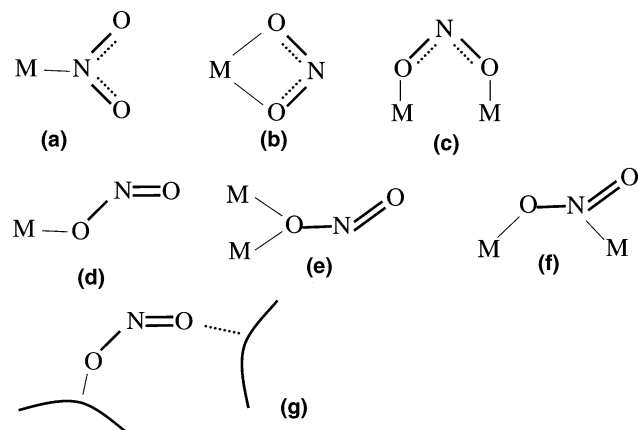


**Figure 4.** Possible adsorption geometries of  $\text{NO}_2$  on SWNTs based on nitrite ion complexes. Structure (a) is a *nitro* configuration, and (b)–(f) are *nitrito* configurations. Structure (g) is a possible adsorption geometry consistent with this work and theoretical calculations.

configurations, but all are bound through at least one O atom. Because N–O bonds in *nitrito* complexes are not necessarily equivalent, they can exhibit dissimilar vibrational frequencies. Finally, the bend vibration has been demonstrated to be mostly insensitive to coordination geometry.<sup>37</sup> Because our data show widely separated stretch vibrations at 1302 and 1026  $\text{cm}^{-1}$ , this suggests that  $\text{NO}_2$  adsorbs on SWNTs in something similar to a *nitrito* geometry. We rule out structures similar to a–c in Figure 4 because, in these structures, the oxygen atoms are in equivalent positions. In such configurations, the N–O stretching vibrations are separated by 50–70  $\text{cm}^{-1}$ ,<sup>30</sup> which is not the case for  $\text{NO}_2$ /SWNTs. Additionally,  $\text{NO}_2$  adsorbed on Au(111) assumes a chelating configuration similar to that shown in Figure 4b. As indicated in Table 3, the vibrational data for this system do not agree with our data. The data that are most similar to this work are for the complex<sup>38</sup> in which the  $\text{NO}_2^-$  are oriented in a *nitrito* configuration similar to Figure 4d.<sup>38</sup> As seen in Table 3, the N–O vibrations have similar separation as  $\text{NO}_2$ /SWNTs, but the absolute frequencies are about 100  $\text{cm}^{-1}$  higher. This suggests that these species are in similar configurations but that the nitrogen–oxygen bonds for  $\text{NO}_2$  adsorbed on SWNTs are weaker than those for  $\text{NO}_2^-$  in the metal complex.

Recent theoretical studies have shown that  $\text{NO}_2$ , like  $\text{NH}_3$ , adsorbs more strongly in an interstitial channel than on the outside of a single nanotube.<sup>6</sup> Although our FTIR data for  $\text{NO}_2$  adsorbed on SWNTs do not provide direct evidence for this, the data are consistent with an adsorption geometry that involves the molecule interacting with multiple nanotubes. Specifically, a  $\text{NO}_2$  molecule adsorbed in a structure similar to that in Figure 4g, or a similar analogue of 4e or 4f, could produce the observed FTIR spectrum. If one oxygen atom in the  $\text{NO}_2$  molecule is closer to a nanotube than the other oxygen atom, the N–O stretches will be significantly different in frequency, as is observed for  $\text{NO}_2$  adsorbed on SWNTs. The fact that we do not observe any vibrations attributable to  $\text{N}_2\text{O}_4$  could be due to molecules adsorbing in interstitial sites. Individual  $\text{NO}_2$  molecules could fit between SWNTs, but  $\text{N}_2\text{O}_4$  molecules are too large to do so.

We finally note that the TPD data for both molecules show very broad distributions. This result is consistent with molecules adsorbed in highly heterogeneous environments, such as within interstitial channels. Molecules adsorbed in such locations could require significant energy input to drive them out, or they could take a finite time between detachment and escape from the interstitial channel. However, the width of the distributions could

also be an artifact of the low pumping speed of the vacuum system. Finally, assuming that both compounds desorb via a first-order process with a preexponential factor of  $10^{13} \text{ s}^{-1}$ , adsorption energies of 106 kJ/mol for ammonia and 114 kJ/mol for  $\text{NO}_2$  are calculated. The desorption of these and other molecules from SWNTs is currently being investigated in detail and will be the subject of a forthcoming paper.

## Conclusions

We have studied the adsorption of  $\text{NH}_3$  and  $\text{NO}_2$  on single-walled carbon nanotubes. The FTIR data suggest that  $\text{NH}_3$  interacts with the nanotubes via both the lone pair of electrons and the H atoms. The lack of adsorption of trimethylamine is probably due to its size, which prevents it from entering the energetically favorable adsorption sites between nanotubes. TPD data confirm that  $\text{NH}_3$  and  $\text{NO}_2$  adsorb molecularly and that  $\text{NO}_2$  is slightly more strongly bound than  $\text{NH}_3$ , in qualitative agreement with theoretical results.<sup>4,6</sup> The vibrational data are consistent with molecules that are adsorbed in interstitial channels in nanotube bundles. Recent theoretical studies indicating that such bonding sites are more energetically favorable lead us to conclude that this is indeed the likely bonding geometry. If so, the use of gases to alter the electrical properties of SWNTs will be more effective for nanotube bundles than for single nanotubes.

**Acknowledgment.** We gratefully acknowledge Karl Johnson for providing us with the coordinates of the C atoms in a heterogeneous bundle of nanotubes from published studies. We also thank R. N. Zare and J. T. Yates, Jr. for useful comments on the manuscript. This work was supported by a Cottrell College Science Award from Research Corporation.

## References and Notes

- (1) Ijima, S. *Nature* **1991**, *354*, 56.
- (2) Kong, J.; Franklin, N. R.; Zhou, C.; Chapline, M. G.; Peng, S.; Cho, K.; Dai, H. *Science* **2000**, *287*, 622.
- (3) Collins, P. G.; Bradley, K.; Ishigami, M.; Zettl, A. *Science* **2000**, *287*, 1801.
- (4) Chang, H.; Lee, J. D.; Lee, S. M.; Lee, Y. H. *Appl. Phys. Lett.* **2001**, *79*, 3863.
- (5) Shi, W.; Johnson, J. K. *Phys. Rev. Lett.* **2003**, *91*, 15504.
- (6) Zhao, J.; Buldum, A.; Han, J.; Lu, J. P. *Nanotechnology* **2002**, *13*, 195.
- (7) Kuznetsova, A.; Yates, J. T.; Liu, J.; Smalley, R. E. *J. Chem. Phys.* **2000**, *112*, 9590.
- (8) Kuznetsova, A.; Yates, J. T.; Simonyan, V. V.; Johnson, J. K.; Huffman, C. B.; Smalley, R. E. *J. Chem. Phys.* **2001**, *115*, 6691.
- (9) Byl, O.; Kondratyuk, P.; Forth, S. T.; FitzGerald, S. A.; Chen, L.; Johnson, J. K.; J. T. Yates, J. *J. Am. Chem. Soc.* **2003**, *125*, 5889.
- (10) Lubezky, A.; Chechelnitsky, L.; Folman, M. *J. Chem. Soc., Faraday Trans.* **1996**, *92*, 2269.
- (11) Fastow, M.; Kozirovski, Y.; Folman, M.; Heidberg, J. *J. Phys. Chem.* **1992**, *96*, 6126.
- (12) Lubezky, A.; Chechelnitsky, L.; Folman, M. *Surf. Sci.* **2000**, *454*–*456*, 147.
- (13) Chiang, I. W.; Brinson, B. E.; Huang, A. Y.; Willis, P. A.; Bronikowski, M. J.; Margrave, J. L.; Smalley, R. E.; Hauge, R. H. *J. Phys. Chem. B* **2001**, *105*, 8297.
- (14) Chiang, W.; Brinson, B. E.; Smalley, R. E.; Margrave, J. L.; Hauge, R. H. *J. Phys. Chem. B* **2001**, *105*, 1157.
- (15) Cinke, M.; Li, J.; Chen, B.; Cassell, A.; Delzeit, L.; Han, J.; Meryappan, M. *Chem. Phys. Lett.* **2002**, *365*, 69.
- (16) Dillon, A. C.; Gennett, T.; Jones, K. M.; Alleman, J. L.; Parilla, P. A.; Heben, M. J. *Adv. Mater.* **1999**, *11*, 1354.
- (17) Rinzler, A. G.; Liu, J.; Dai, H.; Nikolaev, P.; Huffman, C. B.; Rodriguez-Macias, F. J.; Boul, P. J.; Liu, A. H.; Heymann, D.; Colbert, D. T.; Lee, R. S.; Fischer, J. E.; Rao, A. M.; Eklund, P. C.; Smalley, R. E. *Appl. Phys. A* **1998**, *67*, 29.
- (18) Kuznetsova, A.; Mawhinney, D. B.; Naumenko, V.; Yates, J. T., Jr.; Liu, J.; Smalley, R. E. *Chem. Phys. Lett.* **2000**, *321*, 292.

- (19) Georgakilas, V.; Voulgaris, D.; Vazquez, E.; Prato, M.; Guldi, D.; Kukovecz, A.; Kuzmany, H. *J. Am. Chem. Soc.* **2002**, *124*, 14318.
- (20) Prato, M. Personal Communication—Purification; July 2003.
- (21) Rowntree, P.; Scoles, G.; Xu, J. *J. Chem. Phys.* **1990**, *92*, 3853.
- (22) Sjoqvall, P.; Kasemo, S. K. S. B.; Franchy, R.; Ho, W. *Chem. Phys. Lett.* **1990**, *171*, 125.
- (23) Gu, Z.; Peng, H.; Hauge, R. H.; Smalley, R. E.; Margrave, J. L. *Nanoletters* **2002**, *2*, 1009.
- (24) Wanna, J.; Menapace, J. A.; Bernstein, E. R. *J. Chem. Phys.* **1986**, *85*, 1795.
- (25) Menapace, J. A.; Bernstein, E. R. *J. Phys. Chem.* **1987**, *91*, 2533.
- (26) Bredas, J. L.; Street, G. B. *J. Chem. Phys.* **1989**, *90*, 7291.
- (27) Rodham, D. A.; Suzuki, S.; Suenram, R. D.; Lovas, F. J.; Dasgupta, S.; Goddard, W. A.; Blake, G. A. *Nature* **1993**, *362*, 735.
- (28) Talapatra, S.; Migone, A. D. *Phys. Rev. B* **2002**, *65*, 045416.
- (29) Muris, M.; Dufau, N.; Bienfait, M.; Dupont-Pavlovsky, N.; Grillet, Y.; Palmari, J. P. *Langmuir* **2000**, *16*, 7019.
- (30) Nakamoto, K. *Infrared and Raman Spectra of Inorganic and Coordination Compounds*; John Wiley and Sons: New York, 1997.
- (31) Parmeter, J. E.; Wang, Y.; Mullins, C. B.; Weinberg, W. H. *J. Chem. Phys.* **1988**, *88*, 5225.
- (32) Kim, C. S.; Bermudez, V. M.; Russell, J. N. *Surf. Sci.* **1997**, *389*, 162.
- (33) Rodriguez, J. A.; Kuhn, W. K.; Truong, C. M.; Goodman, D. W. *Surf. Sci.* **1992**, *271*, 333.
- (34) Dastoor, H. E.; Gardner, P.; King, D. A. *Surf. Sci.* **1993**, *289*, 279.
- (35) Huang, W. X.; White, J. M. *Surf. Sci.* **2003**, *529*, 455.
- (36) Wang, J.; Koel, B. E. *J. Phys. Chem. A* **1998**, *102*, 8573.
- (37) Cotton, F. A.; Wilkinson, G. *Advanced Inorganic Chemistry*, 5th ed.; John Wiley & Sons: New York, 1988.
- (38) Goodgame, D. M. L.; Hitchman, M. A. *Inorg. Chem.* **1964**, *3*, 1389.
- (39) <http://webbook.nist.gov> (accessed October 2003).
- (40) Binbrek, O. S.; Anderson, A. *Chem. Phys. Lett.* **1972**, *15*, 421.